Available online at www.sciencedirect.com
ScienceDirect
Trans. Nonferrous Met. Soc. China 20(2010) s815−s820
Transactions of Nonferrous Metals Society of China
www.tnmsc.cn

Microstructure evolution behavior of AlSi9Cu3 alloy during rheocasting

GUO Hong-min(郭洪民), LIU Xu-bo(刘旭波), YANG Xiang-jie(杨湘杰), ZHANG Ai-sheng(章爱生), LIU Yong(刘勇)
School of Materials Science and Engineering, Nanchang University, Nanchang 330031, China

Received 13 May 2010; accepted 25 June 2010

Abstract: The experimental and analytical approaches were taken to investigate the non-dendritic microstructure formation and evolution of AlSi9Cu3 alloy during rheocasting. The results show that the globular primary α(Al) particles free of entrapped eutectic form after rheocasting for 3 s, and could be morphologically stabilized during subsequent growth. The fine and globular particles underwent a coarsening process under quiescently continuous cooling in which the particle density decreases, the solid fraction increases, the average particle size increases with the increase of solidification time at a rate that closely followed the classical Ostwald ripening.
Keywords: AlSi9Cu3 alloy; microstructure evolution; rheocasting; interface instability; growth; coarsening

1 Introduction

Since the semi-solid metal (SSM) forming is discovered, most part production is thixocasting in which a particular type of solid feedstock is reheated into the semi-solid range to form non-dendritic slug that is then used in subsequent forming operation. However, it is now evident that rheocasting offers significant advantages of processing semi-solid slurry directly from liquid alloy and recycling scrap metals in-house[1−2]. The desired raw material for rheocasting is partially solidified slurry in which the solid is present as fine and nearly perfect globular particles. This curious microstructure attracts both commercial interest from enhanced mechanical properties and also scientific interest in explaining the mechanism of globular grain formation. It has been claimed that such globular particles can be formed by the fragmentation either through the bending of dendrite arms followed by liquid penetration of the high angle grain boundaries or through remelting at the root of dendrite arms due to direct or indirect agitation during solidification[1–4], such as electromagnetic stirring, mechanical stirring and ultrasonic vibration. Recent researches indicate that the globular particles can form directly from the melt[5–7], and the agitation needs only be applied during the very early stage of solidification[7]. By accomplishing this finding, many novel rheocasting techniques have been developed[8–12], and extensive investigations are being undergone. FAN et al[13–15] examined the solidification behavior of alloys and coarsening of particles under intensive forced convection in the rheodiecasting process. WANNASIN et al[10] evaluated the solid fraction during gas-induced rheocasting process by a rapid quenching method. MARTINEZ et al[16] investigated the spheroidal particle stability in rheocasting.

However, experimental observation of the initial stages of solidification in rheocasting is very limited, although it is critically important for the formation of globular particles. For most of modern rheocasting techniques, the semi-solid slurry is usually handled under quiescently continuous cooling prior to subsequent component shaping, thus it is also important to investigate the stability and extent of coarsening of the particles in order to control the flow behavior of semi-solid slurry in the die cavity. The present work aims at studying microstructure evolution behavior of an AlSi9Cu3 alloy at the early solidification stages.

2 Experimental

The raw material used in this work was a secondary die casting aluminum alloy AlSi9Cu3 (balance Al, 9.4% Si, 3.4%Cu, 0.72%Fe, 0.72%Zn, 0.27%Mn, 0.34%Mg,

Foundation item: Project(50804023) supported by National Natural Science Foundation of China; Project(205084) supported by Ministry of Education Focused on Scientific and Technological Research
Corresponding author: GUO Hong-min; Tel: +86-791-3969611; E-mail: guohongmin@ncu.edu.cn

mass fraction). The temperature vs solid fraction curve of this alloy was determined by thermodynaminc calculation based on the Scheil model. The useful part of the curve (from full liquid to 29% solid fraction) is shown in Fig.1. From Fig.1, the liquidus temperature of the alloy is about 594 °C. Compared with other alloys widely used for investigations on rheocasting, such as A356 aluminum alloy, Al-4.5% Cu and AZ91 magnesium alloy, the slope of solid fraction vs temperature curve of AlSi9Cu3 is not steep, resulting in easy control of solid fraction. Importantly, AlSi9Cu3 solidifies with a much smaller amount of primary solid, which makes it easier to identify particles generated at even shorter solidification time in rheocasting.

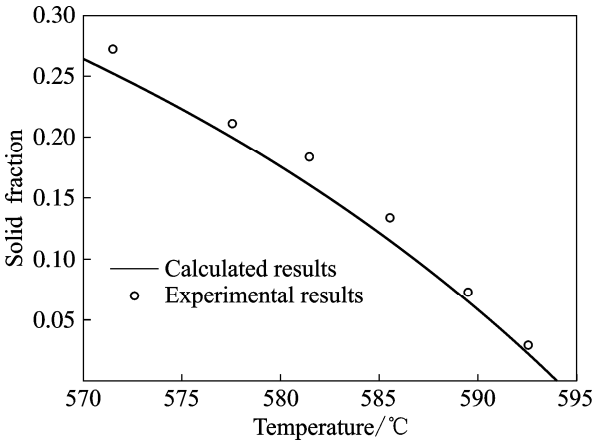

Fig.1 Curves of solid fraction vs temperature of AlSi9Cu3 alloy

The semisolid slurry was produced using LSPSF (low superheat pouring with a shear field) technique[11]. In order to evaluate the microstructure evolution, the quantitative metallography on microstructures quenched from semi-solid state was used. The rapid quenching was utilized by the mold used in conventional high pressure die casting (HPDC, 280 t cold chamber machine). The mold consisted of two thick steel plates forming a channel with thickness of 2 mm, width of 12 mm and length of 20 mm. The shot sleeve was preheated up to 520 °C, the shot speed was set at 5m/s, the size of gate was designed with thickness of 2 mm and width of 12 mm. These measures can effectively reduce the effects of shot sleeve on the semi-solid slurry.

The AlSi9Cu3 alloy was melted in a resistance furnace at 710 °C. A predetermined dose of melt was then cooled to the temperature of (630±3) °C, and was cast over the rotating barrel which rotated at a speed of 90 r/mm, inclined at 20° with respective to the horizontal plane and was operated at a temperature of 200°C. Then, the melt was collected in a slurry holder (coated with boron nitride, preheated up to 570 °C), and underwent coarsening under a quiescent and slower cooling condition. The semi-solid slurry was transferred into the shot sleeve at different time intervals, and immediately injected into the thin mold rapidly under pressure. The high cooling rate achieved by the mold allowed the capture of the microstructure at semi-solid state. In this work, liquid alloy flowed through the rotating barrel within 3 s and the temperature of melt was decreased to about 592 °C. Six levels of solid fractions were obtained by varying the slower cooling durations (coarsening times) of 0 s(at 592 °C), 15 s(at 589 °C), 42 s(at 585 °C), 82 s(at 581 °C), 110 s(at 578 °C) and 300 s(at 571 °C).

Samples for microstructure examination were cut from the middle location of the quenched plate, prepared by the standard metallurgical technique and followed by etching with the Keller's reagent. The microstructure was examined by a Zeiss optical microscope equipped with image quantitative analysis system. The particle size, shape factor, particle density and solid fraction of the primary α(Al) were measured. The diameter (D) was calculated as the diameter of a circle having the same area as that of the particles in the micrograph. The solid fraction after quenching (f) was calculated using

$$f=\frac{\sum_{i=1}^{N}A_i}{A_T} \tag{1}$$

where A_i is the solid particle area for particle I; A_T is the analyzed area; N is the total number of examined solid particle. The shape factor (SF) is defined as

$$SF=\frac{1}{N}\sum_{i=1}^{N}\frac{4\pi A_i}{P_i^2} \tag{2}$$

where P_i is the solid particle peripheral length for particle i. Particle density (N_v) was calculated using

$$N_v=\frac{f}{\frac{4}{3}\pi\left(\frac{D}{2}\right)^3} \tag{3}$$

3 Results and discussion

The solid fractions in semi-solid microstructures as shown in Fig.2, measured according to Eq.(1) are plotted in Fig.1. The solid fractions obtained from quantitative metallography of quenched plates are slightly higher than the theoretical calculated ones. Similar results exhibit that such an overestimation of the solid fraction has been reported by other investigations [10,17]. The possible reason may be analyzed as follows: 1) No diffusion in the solid is assumed in Scheil mold, which is difficult to attain in the present rheocasting. During the quiescent

cooling, there is enough time for homogenization, resulting in an overestimated value of solid fraction[17]. 2) The inevitable experimental errors correlate with time in the practical operation. In summary, the present rapid quenching mold is an effective tool to evaluate the solid fraction. Thus, it can be used to capture the microstructure before quenching to evaluate the microstructure evolution in semi-solid state.

3.1 Grain formation during earliest stage of solidification

It is very difficult to determine the solidification time below the liquidus temperature achieved by the melt when it flows through the rotating barrel. The experimental investigations on Al-Si and Al-Cu alloys show that the average particle radius in rheocast alloys change as the cube root of the solidification time at roughly the same rate as dendrite arm spacing (DAS) does in dendrite alloys[7,18–19]. Therefore, it can approximately estimate the local solidification time for the primary α(Al) in AlSi9Cu3 alloy. As the average particle size of primary α(Al) in Fig. 2(a) is measured to be 14μm in diameter, it gives a local solidification time of about 3s according to the previous measurement[7].

Figs.2(a)–(d) show the rheocast microstructure, of AlSi9Cu3 quenched into the mold after being slower cooling for 0, 42, 110 and 300 s, respectively. The time started from the completion of transfer from the rotating barrel into the slurry holder. After rheocasting for 3 s (Fig.2(a)), near globular particles form, the distribution of solid particles are uniform and most of them are dispersed separately in the liquid matrix, the particle density calculated from Eq.(3) is about 2.0×10^4 /mm^3.

Crucial conditions to change microstructure using LSPSF are highly localized chill resulted from contacting the melt using rotating barrel and exerted violent convection as a result of gravity force and rotation of barrel[11]. The melt introduced into the rotating barrel has zero rotation speed, and then the speed tends to increase by friction and centrifugal forces, but the inertia and gravity force restrain this tendency, resulting in a relative movement between the melt and the barrel wall. In addition, the gravity force pushes and accelerates the melt to flow along the axial direction of the inclined barrel, resulting in another relative movement. Driven by these relative movements, the region near the solid-liquid interface suffers a violent turbulent flow and shear stress. When the melt is flowing over the surface of the rotating barrel, there is an enormous amount of ever-changing interfacial area between the solidifying alloy and the rotating barrel, which can provide an enhanced heat transfer to enhance the heterogeneous nucleation formed on or adjacent to the surface of the rotating barrel[20–21]. The violent convection due to the relative movements

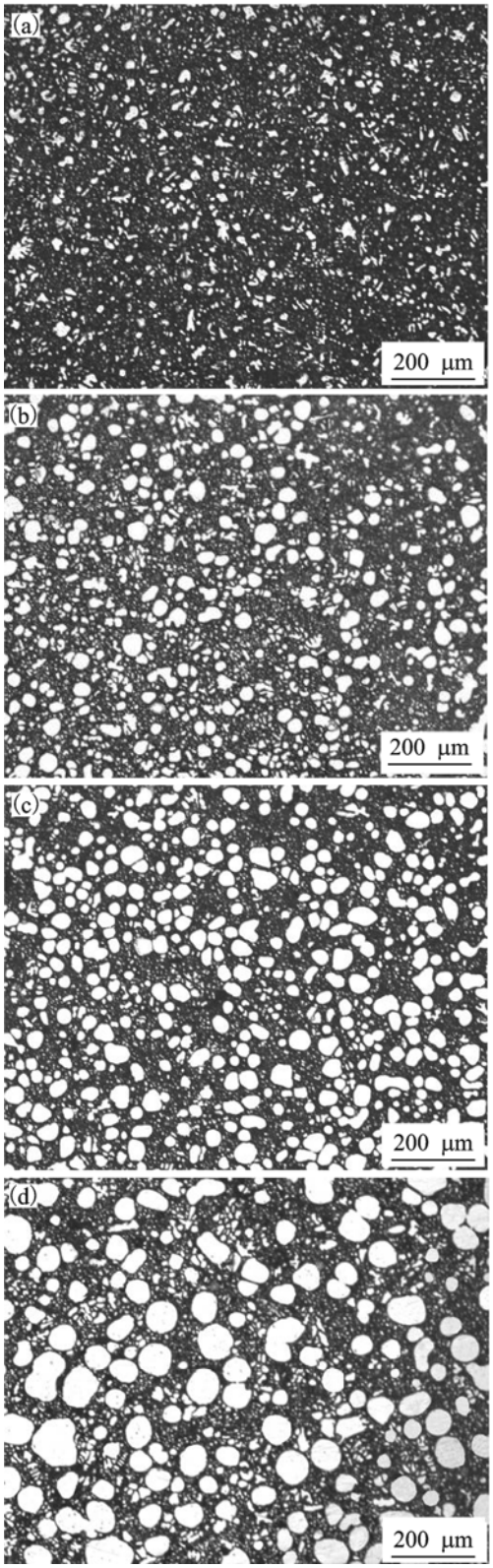

Fig.2 Microstructures evolution of primary α(Al) during slower cooling in slurry holder: (a) 592 °C, 0 s; (b) 585 °C, 42 s; (c) 578 °C, 110 s; (d) 571 °C, 300 s

leads to the detachment of formed crystals from the barrel wall or the breaking of dendrites formed in the thermal undercooled region adjacent to the barrel

wall[1,21]. Due to the continuous localized chill, the bulk melt temperature is decreased below the liquidus temperature, enhancing the survival of the formed free primary solid phase. These will result in the formation of a high density of grain well distributed in the melt just below the liquidus temperature. However, it is not possible from present work to determine the morphology and formation for rheocasting times shorter than 3 s. Useful information will be obtained by future work which aims at working on rheocasting experiments with transparent analogue systems.

3.2 Coarsening during continuous cooling

With prolonged quiescently slower cooling (Figs.2 (b)-(d)), no agglomeration was observed and most of the solid particles were isolated. These particles show no sign of entrapped eutectic at different stages. The effects of quiescent cooling time on the particle size, particle density and shape factor are shown in Fig.3. The time starts from the completion of transfer from the rotating barrel into the slurry holder. From Fig.3, the variation in shape factor is not significant. Average particle size increases with cooling time increasing, which responses to the decrease of particle density.

The kinetic of grain growth in the in semi-solid state have been shown to approximate to a diffusioncontrolled

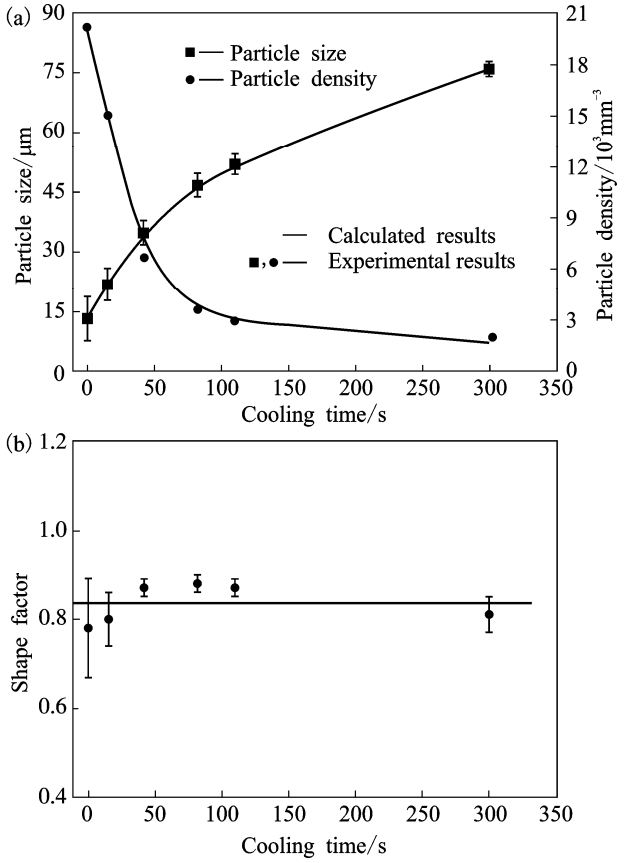

Fig.3 Effects of slower cooling time in slurry holder on particle density and particle size (a) and shape factor (b)

coarsening[19, 22–23]. The coalescence and Ostwald ripening generally control grain coarsening, and Ostwald repining is the main mechanism when the liquid fraction is relatively high[19]. In accordance with our observations (Figs.2–3), the coarsening of particles in the semi-solid slurry obeys Ostwald ripening. In the theory of Ostwald repining, the classical Lifshitz-Slyozov-Wagner (LSW) can be used to describe the time dependency of the grain growth[24–25].

$$d^n - d_0^n = Kt \tag{4}$$

where d_0 is the initial particle size; d is the size at time of t; n is the coarsening exponent; K is the coarsening rate constant. The experimental data in Fig.3 are reconstructed according to Eq. (4) at n=3 and the result is shown in Fig.4. The coarsening rate constant is 181 μm^3/s. The resulted regression coefficient values (R^2) is very close to 1, indicating that the experimental data are well fitted to the LSW at $n=3$ and the coarsening is mainly volume diffusion-controlled. It should be noted that the coarsening in the present work happens under a slower cooling, but not isothermal condition. One assumption of the LSW is that the diffusion fields surrounding the particles do not overlap[19,26]. Thus, LSW is more suitable for the coarsening of isolated globular particles. For AlSi9Cu3 alloy, the solid fraction is much lower, resulting in a larger space between particles. Moreover, the cooling rate occurring in the present coarsening is very small. Under these conditions, LSW can be used to describe the coarsening of fine and globular particles in semi-solid slurry of AlSi9Cu3 alloy under slower cooling. This provides an effective way to estimate the particle size in semi-solid slurry of AlSi9Cu3 alloy for industrial applications.

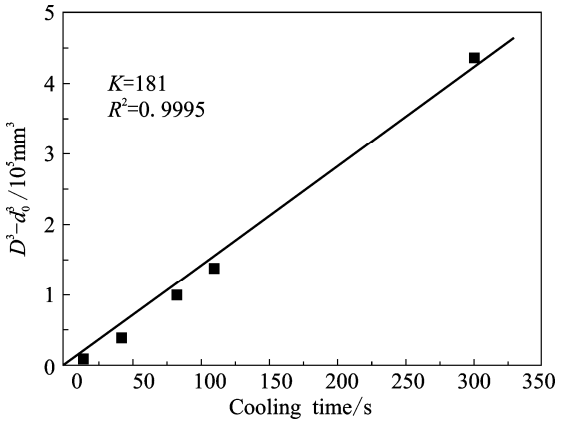

Fig.4 Evolution of average particle diameter as function of cooling time

The Ostwald ripening mechanism is driven by the presence of variable curvature of different particles. It is easily concluded that the smaller primary α(Al) grains with size below average diameter dissolved gradually but

the larger primary α(Al) grains with size above average diameter grow, and the particle density decreases. A notable point which can be deduced from Fig.3 is that the standard deviations of shape factor and particle size are large at the beginning of quiescent cooling, and decrease with increasing the cooling time. Thus, the driving force of Ostwald ripening is large at the beginning of quiescent cooling, resulting in a rapid coarsening and significant decrease of particle density. With the cooling time increasing, the particles have morphology close to globular and particle size with a narrow distribution around the average diameter (Fig.3). The solid line represents the curve fitted to the classical SLW equation at $n=3$. R_2 is the regression coefficient. Consequently, the driving force for Ostwald ripening is obviously decreased, resulting in a slow coarsening.

3.3. Particle stability during rheocasting

The formed primary α(Al) particles remain globular morphology during the slower cooling stage with a shape factor as large as 0.78–0.88. The Mullins-Sekerka (M-S) instability theory[27] points out that the stability of the solid-liquid interface under the condition of pure diffusion is controlled by the temperature gradient, solute concentration gradient and surface energy. Based on this, Langer developed a stability criterion for growth of a three dimensional globular interface in the melt[28].

$$R_c = \left(\frac{30 D_L \Gamma}{m_L C_0 (k-1) v} \right)^{\frac{1}{2}} \tag{5}$$

where R_c is the critical particle radius; C_0 is the bulk solute concentration; D_L is the solute diffusivity in liquid phase; Γ is the Gibbs-Thompson coefficient; m_L is the slope of the liquidus line; k is the alloy partition coefficient; v is the interface velocity. The average interface velocity, v, for growth up to the measured radius $R_m=D/2$ was estimated by dividing R_m by the total time the alloy was below the liquidus temperature before quenching.

$$v = \frac{R_m}{t} \tag{6}$$

As mentioned before, the solidification time of primary α(Al) shown in Fig.2(a) is about 3s. Based on Eq.(6), the growth velocities after 3, 18, 45, 85, 113 and 303s can be obtained. The measured radius and estimated growth velocities are plotted on the standard stability criterion curve using property values from Table 1[29–30], as shown in Fig.5. All of points are in the stable region. It is now accepted that if the formed particles are sufficiently high in number density, subsequent growth of these particles is non-dendritic[19]. The number of growing particles of rheocasting in present rheocasting was about 2×10^4/mm^3 after 3 s, and about 3×10^3/mm^3 after 113 s. Under such high particle density formed in the initial stage of solidification, for a given increase in solid fraction during cooling, each particle only needs to grow a small amount. This will favor globular growth and dendrite growth is suppressed. The experimental results from A356 and Al-20%Cu (mass fraction)[11,31] show that dendritic or rosette-like primary particles are characterized by a very small particle density in the semi-solid microstructures. Under the effect of the shot sleeve, the standard deviation of shape factor in Fig.2(a) is relatively large, which indicates that the morphologies of some particles are not regular with higher interface energy. The subsequent slower cooling can further reduce the total surface energy through mass diffusion from regions of high interfacial curvature to low interfacial curvature. As the shape of particles is fairly globular, the long-range coarsening between different particle sizes is the main mechanism to decrease surface energy. The particle morphology is changed by dissolving smaller particles and transferring their mass to the larger ones. The numerical simulation of LSPSF rheocast microstructure show that at higher solid fraction, when particles are larger and less distanced from each other, the gradient of solute concentration in front of solid-liquid interface decreases rapidly due to the soft impingement of the solute diffusion layers around particles[31]. If the higher density of primary particle forms in the earliest stage of solidification, the possibility of soft impingement increases due to the decreased particle spacing. Under these situations, the growth velocity of particles is significantly reduced, and the particles can retain globular growth throughout of the quiescently slower cooling.

Table 1 Thermochemical and physical properties of solid and liquid at melting points[29-30]

T_m/K	D_L/(m^2 • s^{-1})	m_L/%	K	C_0/%	Γ/km
933.5	3×10^{-9}	−6.5	0.13	9.4	1.96×10^{-7}

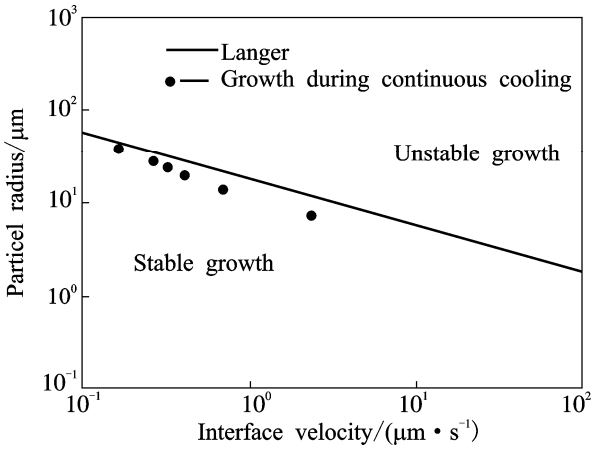

Fig.5 Stable particle size from experimental data in comparison with Langer interface stability criterion

4 Conclusions

1) The present rapid quenching is an effective tool to evaluate the solid fraction and microstructure evolution in the semi-solid state.
2) The fine and globular particles were observed in AlSi9Cu3 alloy quenched after rheocasting for 3 s, and can maintain morphologically stabilized during quiescently slower cooling.
3) The particle coarsening occurs through Ostwald repining by consumption of smaller particles, and can be described by the classical LSW theory.

References

[1] FLEMINGS M C. Behavior of Metal in the Semi-Solid State [J]. Metall Trans, 1991, 22A: 957−981.
[2] FAN Z. Semisolid metal processing [J]. Inter Mater Rev, 2002, 47: 1−37.
[3] YANG Z, KANG C, SEO P K. Evolution of the rheocasting structure of A356 alloy investigated by large-scale crystal orientation observation [J]. Scripta Mater, 2005, 52: 283−288.
[4] WU S, XIE L, ZHAO J, NAKAE H. Formation of non-dendritic microstructure of semi-solid aluminum alloy under vibration [J]. Scripta Mater, 2008, 58: 556−559.
[5] LI T, LIN X, HUANG W D. Morphological evolution during solidification under stirring [J]. Acta Mater, 2006, 54: 4815−4824.
[6] JI S, FAN Z. Solidification behavior of Sn-15 Wt Pct Pb alloy under a high shear rate and High intensity of turbulence during semisolid processing [J]. Metall Mater Trans, 2002, A33: 3511−3520.
[7] MARTINEZ R A, FLEMINGS M C. Evolution of particle morphology in semisolid processing [J]. Metall Mater Trans, 2005, A36: 2205−2210.
[8] APELIAN D, PAN Q Y, FINDO M. Low cost and energy efficient methods for the manufacture of semi-solid (SSM) feedstock [J]. Die Casting Engineer, 2004, 48(1): 22−28.
[9] LANGLAIS J, LEMIEUX A. The SEED technology for semi-solid processing of aluminum alloys: a metallurgical and process overview [J]. Solid State Phenom, 2006, 116/117: 472−477.
[10] WANNASIN J, CANYOOK R, BURAPA, SIKONG L, FLEMINGS M C. Evaluation of solid fraction in a rheocast aluminum die casting alloy by a rapid quenching method [J]. Scripta Mater, 2008, 59: 1091−1094.
[11] GUO H M, YANG X J. Efficient refinement of spherical grains by LSPSF rheocasting process [J], Mater Sci Technol, 2008, 24: 55−63.
[12] BIROL Y. Internal cooling to produce aluminium alloy slurries for rheocasting [J]. J Alloys Compd, 2009, 480: 365−368.
[13] FAN Z, LIU G. Solidification behaviour of AZ91D Mg-alloy under intensive forced convection in the RDC process [J]. Acta Mater, 2005, 53: 4345−4357.
[14] HITCHCOCK M, WANG Y, FAN Z. Secondary solidification behaviour of the Al-Si-Mg alloy prepared by the rheo-diecasting process [J]. Acta Materialia, 2006, 55: 1589−1598.
[15] JI S, ROBERT K, FAN Z. Isothermal coarsening of fine and spherical particles in semisolid slurry of Mg-9Al-1Zn alloy under low shear [J]. Scripta Mater, 2006, 55: 971−974.
[16] MARTINEZ R A, KARMA A, FLEMINGS M C. Spheroidal particle stability in semisolid processing [J]. Metall Mater Trans, 2006, A37: 2807−2815.
[17] TZIMAS E, ZAVALIANGOS. Evaluation of volume fraction of solid in alloys formed by semisolid processing [J]. J Mater Sci, 2000, 35: 5319−5329.
[18] REISI M, NIROUMAND. Growth of primary particles during secondary cooling of a rheocast alloy [J]. J Alloys Compd, 2009, 470: 413−419.
[19] FLEMINGS M C. Coarsening in solidification [J]. Mater Trans, 2005, 46: 895−900.
[20] FALAK P, NIROUMAND. Rheocasting of an Al–Si alloy [J]. Scripta Mater, 2005, 53: 53−57.
[21] OHNO A. Solidification: The Separation Theory and its Practical Applications [M]. Berlin: Springer-Verlag, 1987.
[22] LOUE W R, SUERY M. Microstructural evolution during partial remelting of Al-Si7Mg alloys [J]. Mater Sci Eng, 1995, A203: 1−13.
[23] ATKINSON H V, LIU D. Microstructural coarsening of semi-solid aluminium alloys [J]. Mater Sci Eng, 2008, A496: 439−446.
[24] LIFSHITS I M, SLYOZOV V V. The kinetics of precipitation from supersaturated solid solutions [J]. Phys Chem Solids, 1961, 19: 35−50.
[25] WAGNER C. Theorie der Alterung von Niederschlagen dursch Umlosen (Ostwald-Reifung) [J]. Z. Electrochem, 1961, 65: 581−586.
[26] BALDAN A. Progress in Ostwald ripening theories and their applications to Nickel-Base Superalloys [J]. J Mater Sci, 2002, 37: 2171−2202.
[27] MULLINS W W, SEKERKA R F. Morphological stability of a particle growing by diffusion or heat flow [J]. J Appl Phys, 1963, 34: 323−329.
[28] LANGER J S. Instabilities and pattern formation in crystal growth [J]. Rev Mod Phys, 1980, 52: 1−27.
[29] GEER A L, ANUNN M, TRONCHE A, EVANS P V, BRISTOW D J. Modelling of inoculation of metallic melts: Application to grain refinement of aluminium by Al-Ti-B [J]. Acta Mater, 2000, 48: 2823−2835.
[30] BRANDES E A, BROOK G B. Smithells metals reference book [M]. Oxford: Butterworth, 1992.
[31] GUO H M, YANG X J. Morphology evolution of primary particles in LSPSF rheocasting process [J]. Inter J Mod Phys B, 2009, 23: 881−887.

(Edited by LI Yan-hong)